Methanol Reaction with Sulfuric Acid: A Vibrational Spectroscopic Study

Lisa L. Van Loon and Heather C. Allen*

Department of Chemistry, The Ohio State University, 100 West 18th Avenue, Columbus, Ohio 43210

Received: May 27, 2004; In Final Form: August 19, 2004

The reaction between methanol and sulfuric acid (SA) was investigated using Raman and vibrational broad bandwidth sum frequency generation spectroscopies. Evidence for the formation of methyl hydrogen sulfate (MHS) was obtained by the presence of a new peak in the 800 cm^{-1} region, not present in either the neat methanol or concentrated sulfuric acid spectra. This peak is attributed to the singly bonded OSO symmetric stretch of MHS. The maximum yield of MHS with a large SA excess (7 SA/1 methanol) is shown to be (95 ± 5)% at −(15 ± 2) °C. No evidence was found to suggest formation of dimethyl sulfate.

Introduction

The uptake of methanol by sulfuric acid solutions has recently been studied,[1,2] and the "esterification" of methanol by sulfuric acid has been known since the 1950s.[3] Yet, direct measurement of the reaction products has remained elusive. We present spectroscopic evidence of the formation of methyl hydrogen sulfate (CH$_3$OSO$_3$H) using Raman spectroscopy to investigate the bulk solution. Surface studies are also presented. Surface tension measurements provide a macroscopic understanding of the surface, and broad bandwidth sum frequency generation (BBSFG) spectra present a molecular view of the surface.

This work was initially motivated by an interest in understanding atmospheric aerosol chemistry since the reaction between sulfuric acid aerosols and tropospheric methanol is not well understood at the molecular level. To simplify the experimental conditions, concentrated (∼96 wt %) sulfuric acid was used to minimize the presence of water in these studies. Lower sulfuric acid concentrations, while more relevant to tropospheric aerosol conditions, are beyond the scope of this work.

Chemical abbreviations used in this paper are MeOH (methanol); SA (sulfuric acid); MHS (methyl hydrogen sulfate); DMSO$_4$ (dimethyl sulfate).

Raman and Sum Frequency Spectroscopies. Raman and sum frequency generation (SFG) vibrational spectroscopies were used to elucidate the bulk reaction and surface structure of the methanol with concentrated sulfuric acid reaction. Raman spectroscopy was used to follow the vibrational signatures of the reactants and products and was selected here as an appropriate tool for this task since it can be used on samples contained in laboratory glassware with minimal spectral interference. Raman scattering is based on changes in polarizability of a vibration as opposed to changes in dipole moment as in IR spectroscopy. This gives rise to different vibrational intensities and allowed modes as compared to IR spectra. For the surface spectra, sum frequency generation spectroscopy was used and is briefly discussed below. SFG is proportional to the Raman and IR transition moments, yet is surface selective.

Sum frequency generation is a second-order nonlinear optical technique sensitive to environments lacking inversion sym-

metry. It has been used to study a variety of solid[4–8] and liquid surfaces[9–17] including those with atmospheric relevance.[6,10–13,15,18–21] SFG is sensitive to both the molecular orientation at the interface and the number density, *N*. A brief introduction to the theory of SFG follows, and more thorough treatments can be found elsewhere.[22–29]

The macroscopic nonlinear susceptibility, $\chi^{(2)}$, is described by a nonresonant term, $\chi^{(2)}_{NR}$, and the sum of the resonant terms, $\chi^{(2)}_\nu$, eq 1.

$$|\chi^{(2)}|^2 = |\chi^{(2)}_{NR} + \sum_\nu \chi^{(2)}_\nu|^2 \tag{1}$$

The resonant response dominates when the frequency of the incident infrared beam, ω_{IR}, is resonant with the ν vibration in the system. It is proportional to the strength of the transition moment, A_ν, as shown in eq 2.

$$\chi^{(2)} \propto \frac{A_\nu}{\omega_\nu - \omega_{IR} - i\Gamma_\nu} \tag{2}$$

A_ν includes both Raman and infrared contributions, meaning SFG is observed when the vibrational transition is both Raman and infrared active. The center frequency of the transition moment is ω_ν, and the line width of the transition is described by Γ_ν.

The intensity of the SFG, I_{SFG}, is proportional to the absolute square of $\chi^{(2)}$ and the intensity of both incident beams, eq 3.

$$I_{SFG} \propto |\chi^{(2)}|^2 I(\omega_{IR})I(\omega_{800}) \tag{3}$$

Experimental Section

Methanol (HPLC grade), sodium methyl sulfate (99%), dimethyl sulfate (99+ %), sulfuric acid (96.6 wt %), and hydrochloric acid (trace metal grade) were used as received. Nanopure water (17.8–18.3 MΩ·cm) was used. The only water present in the methanol–sulfuric acid reaction system was brought in with the addition of the 96.6 wt % sulfuric acid. To completely dissolve CH$_3$OSO$_3$Na in SA, solution vials were placed in a warm water bath. Spectra peak positions were fit using IgorPro 4.05. Fits were made using a Voigt shape with background correction.

* To whom correspondence should be addressed. E-mail: allen@chemistry.ohio-state.edu.

Methanol Reaction with Sulfuric Acid

J. Phys. Chem. B, Vol. 108, No. 45, 2004 **17667**

In the low temperature study, a vial containing 96.6 wt % sulfuric acid was placed in a freezer at $-(15 \pm 2)$ °C to temperature-equilibrate and was stirred. MeOH (1.00 mL) was delivered to the vial (1.37 molal, m), and Raman spectra were acquired every minute for a minimum of 12 h. The room temperature study was conducted at (23 ± 1) °C beginning with cold sulfuric acid and methanol since mixing is exothermic. The high temperature study was conducted by mixing cold sulfuric acid and methanol in a water bath, and Raman spectra were obtained before mixing with a stir-bar began; the solutions were stirred and then heated in an oven to (82 ± 2) °C for several days. In the high temperature study, spectra were obtained until peak intensities did not change, revealing that reactions had come to completion.

Surface Tension Measurements. Surface tension measurements were made using the Kibron Inc. μ-trough system, based on the Wilhelmy plate technique, with DeltaGraph v 2.15 software. Solution (1.00 mL) was delivered into a PTFE tray for each measurement. The temperature varied between 26.0 and 28.7 °C.

Ab Initio Calculations. Calculations were performed using Gaussian 03 for Windows;[30] the 6-31+G** basis set was chosen for all ab initio calculations.[31]

Raman Instrumentation. Raman spectra were obtained using 120−225 mW depending on the experiment from a 785 nm continuous wave laser (Raman Systems Inc). The backscattered light was collected by a fiber optic probe (Inphotonics) coupled to the entrance slit of a 500-mm monochromator (Acton Research, SpectraPro 500i) using a 600 groove/mm grating blazed at 1 μm. The slit width was set to 20 μm, and the band-pass varied between 2.142 cm^{-1} (at 400 cm^{-1}) and 1.503 cm^{-1} (at 3300 cm^{-1}). The spectra were collected in 60 s exposures to a liquid nitrogen cooled CCD camera (Roper Scientific, LN400EB, 1340 × 400 pixel array, back-illuminated and deep depletion CCD). CCD calibration was completed using the 435.833 nm line from a fluorescent lamp.

Calibration of the wavenumber position was completed for each set of experiments by taking a spectrum of crystalline naphthalene and comparing peak positions with the literature values.[32]

SFG Instrumentation. The Allen Lab BBSFG[6,9,10,12,33] system uses a broad bandwidth IR beam (~600 cm^{-1} bandwidth, ~100-fs pulse duration). The SFG system consists of two regenerative amplifiers (Spectra Physics (SP), Spitfires) seeded with sub-50 fs, 800 nm pulses from a Ti:sapphire oscillator (SP, Tsunami) and pumped by a Nd:YLF (SP, Evolution 30) operating at a kHz repetition rate. One amplifier produces 85 fs, 800 nm broadband pulses (~300 cm^{-1}) that are then transformed into a broadband infrared beam in an optical parametric amplifier (SP, OPA-800C). The second amplifier is equipped with a mask to spectrally narrow the 800 nm pulse, 17 cm^{-1}, ~2 ps. (Air−liquid spectra were also obtained with an ~5 cm^{-1} bandwidth;[12] no improvement of resolution was observed, indicating that the line width is limited by the chemical system.) The infrared pulse energy used was 10 μJ, and the visible pulse energy was 115 μJ. The two beams overlap spatially and temporally on the liquid surface of interest, and the resulting sum frequency beam enters the 500 mm monochromator with the slit width set to 3 mm. The beam waist of the focused SFG beam limits the monochromator resolution. The spectrum is dispersed spectrally in the monochromator using a 1200 g/mm diffraction grating blazed at 750 nm (Acton Research, SpectraPro 500i), and the dispersed SF light is collected with a LN$_2$-cooled CCD camera (Roper Scientific, LN400EB, 1340 × 400 pixel array, back-illuminated CCD).
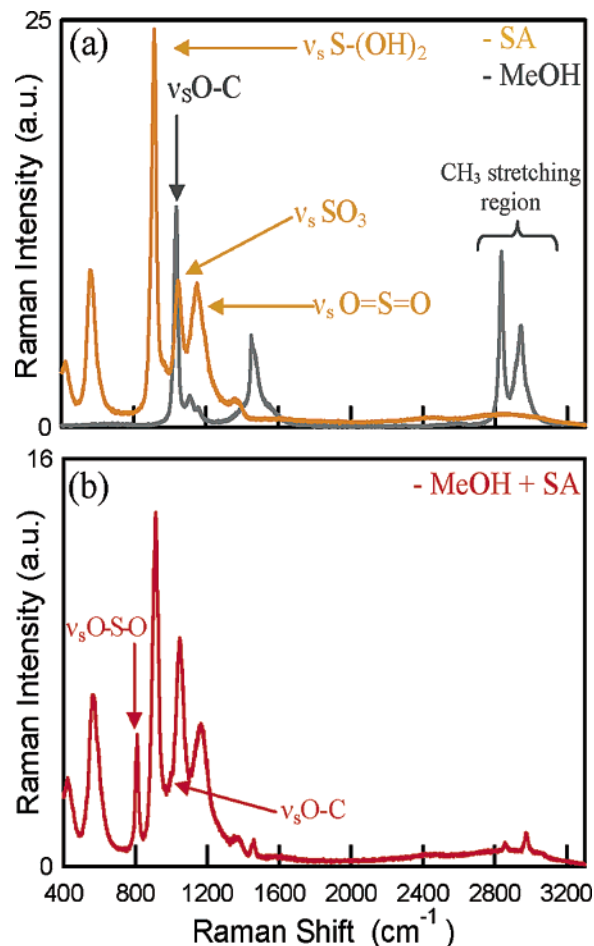
Figure 1. Raman spectra of (a) methanol (grey) and sulfuric acid (gold), and (b) the reaction mixture of methanol + sulfuric acid (red).

Spectra were obtained by integration of the SFG signal for 1−5 min depending on the experiment.

Calibration of the BBSFG system uses a spectrum of GaAs obtained with the IR beam attenuated by passing it through a polystyrene thin film prior to beam overlap on the GaAs. The peak positions (dips) in the polystyrene−GaAs BBSFG spectrum are used to calibrate the spectra. Prior to collecting the BBSFG spectra from the solutions, a nonresonant BBSFG spectrum from the surface of a GaAs crystal is obtained. It is then used to normalize the BBSFG spectra.

SSP polarization conditions were used for the BBSFG spectra shown here. However, SPS polarization conditions were used for additional analysis. The SSP polarization combination probes the isotropic Raman response and the infrared-active dipole moment that is perpendicular to the surface, whereas the SPS polarization condition probes the anisotropic Raman response and the IR transition moment in the plane of the interface. S and P polarized light denotes light that is polarized perpendicular and parallel to the plane of incidence, respectively. SSP or SPS by convention is listed in the following order: SFG, incident visible, and incident IR light.

Results and Discussion

Before studying the reaction of MeOH with SA, it was important to understand the spectroscopic signatures of neat MeOH and SA. Therefore, the liquid Raman spectra of neat methanol and sulfuric acid were obtained, and these spectra are shown in Figure 1a. Their peak assignments are found in Table

TABLE 1: Raman Spectra Peak Assignments for Neat Methanol, 96.6 wt % Sulfuric Acid, Methyl Hydrogen Sulfate in SA, Dimethyl Sulfate in SA, and the Reacted MeOH−SA Solution[a]

peak (cm⁻¹) MeOH[46]	MeOH in HCl	assignment	peak (cm⁻¹) 96.6 wt % SA	assignment
	1003	ν_s O−C of $CH_3OH_2^+$ [35]	417	torsion[47,48]
1034		ν_s O−C	564	S=O_2 rock and bend[47−49]
1111	1100	γ CH_3	912	in-phase stretching S−(OH)$_2$ of H_2SO_4 [34]
1451		δ_s CH_3	969	ν_{as} S−(OH)$_2$ [50]
1470	1461	δ_{as} CH_3	1044	ν_s SO_3 of HSO_4^- in $(HSO_4^-)(H_2SO_4)$[34]
1544		ν O−C + δ O−H···O	1153	ν_s O=S=O[50]
2835	2851	ν_s CH_3	1369	ν_{as} O=S=O[50]
2920	2912	FR (ν_s CH_3 + 2 δ CH_3)[12]		
2944	2958	FR (ν_s CH_3 + 2 δ CH_3)[12]		
2977		ν_{as} CH_3		
	3009	ν_{as} CH_3		

peak (cm⁻¹) MHS in SA[51]	DMSO$_4$ in SA[38]	assignment	peak (cm⁻¹) 7SA/1MeOH	assignment
414	419	torsion (SA)	419	torsion (SA)
	503	δwag O=S=O (DMSO$_4$)		
565	565	S=O_2 rock and bend (SA)	569	S=O_2 rock and bend (SA)
807	769	ν_s O−S−O (DMSO$_4$, MHS)[51,52]	808	ν_s O−S−O (MHS)
909	910	in-phase S−(OH)$_2$ (SA)	912	in-phase S−(OH)$_2$ (SA)
			995	ν_s O−C (MHS)*
1044	1046	ν_s SO_3 (SA)	1046	ν_s SO_3 (SA)
1164	1158	ν_s O=S=O (SA)	1164	ν_s O=S=O
	1197	ν_s O=S=O (DMSO$_4$)		
1371	1367	ν_{as} O=S=O (SA, MHS*, and DMSO$_4$)	1369	ν_{as} O=S=O
			1445	δ_s CH_3 (MHS)
1457	1457	δ CH_3	1459	δ_{as} CH_3 (MHS)
2860	2859	ν_s CH_3	2859	ν_s CH_3 (MHS)
2976	2976	FR (ν_s CH_3 + 2 δ CH_3)*	2975	FR (ν_s CH_3 + 2 δ CH_3)*
3043	3050	ν_{as} CH_3	3047	ν_{as} CH_3 (MHS)

[a] Symbols used in the table are FR = Fermi resonance, ν = stretch, γ = torsion, and δ = deformation modes. The resolution of the peaks is ±2 cm⁻¹. Asterisk (*) denotes assignment by the authors.

1. Of particular interest to this study in the methanol spectrum is the peak at 1034 cm⁻¹ assigned as the symmetric O−C stretch, and the peak at 2835 cm⁻¹ attributed to the CH_3 symmetric stretch. Also, the 2920 cm⁻¹ shoulder and the peak at 2944 cm⁻¹ are assigned to two Fermi resonances. The high energy side of the 2944 cm⁻¹ peak has a shoulder at 2977 cm⁻¹ attributed to the CH_3 asymmetric stretching modes.

The 96.6 wt % SA solution contains both H_2SO_4 and HSO_4^- molecules with the bisulfate ion solvated by multiple H_2SO_4 molecules.[34] Three SA peaks shown in Figure 1a are of particular interest to this study. The peak at 912 cm⁻¹ is attributed to the in-phase symmetric stretching of S(OH)$_2$ from H_2SO_4. The 1044 cm⁻¹ peak is assigned to the SO_3 symmetric stretch of HSO_4^- in the $(HSO_4^-)(H_2SO_4)$ complex. The peak at 1153 cm⁻¹ is assigned to the O=S=O symmetric stretch.

The reacted mixture of methanol with sulfuric acid (7 SA/1 MeOH/1 H_2O) is shown in Figure 1b. Because of the high concentration of SA, it is difficult to distinguish between O−S vibrations due to any reaction product and SA in the region between 400 and 1500 cm⁻¹ since the peaks appear at approximately the same wavenumbers. However, in Figure 1b a peak at 808 cm⁻¹ is observed; this peak is not present in either the neat MeOH or the 96.6 wt % SA spectra (Figure 1a) and is attributed to the singly bonded OSO symmetric stretch of a new species, methyl hydrogen sulfate (CH_3OSO_3H, MHS). The spectrum of an MHS standard solution is shown in Figure 3. In addition to the 808 cm⁻¹ peak in Figure 1b, the shoulder on the low energy side of the SO_3 symmetric stretch peak of SA observed at 995 cm⁻¹ is of interest to this study and is assigned to the O−C symmetric stretch of MHS. This peak is shifted to lower energy as compared to the methanol O−C symmetric stretch (1034 cm⁻¹).

The CH_3 stretching region in the MeOH + SA spectrum of Figure 1b is different from that of neat MeOH. The entire methyl stretch region of Figure 1b is shifted to higher energy relative to the neat MeOH spectrum of Figure 1a. Like for methanol, the 2859 and 2975 cm⁻¹ peaks are assigned to the CH_3 symmetric stretch and a Fermi resonance with the smallest peak at 3047 cm⁻¹ assigned to the CH_3 asymmetric stretching modes. All peak assignments for spectra of Figure 1 are shown in Table 1.

The relative peak intensities in the CH_3 stretching region are also different in the reacted mixture of MeOH + SA compared to the neat methanol spectrum as shown in Figure 1. In addition, the relative intensity of the methanol CH_3 symmetric stretch (2835 cm⁻¹) to the Fermi resonance (2944 cm⁻¹) is 2:1 in the methanol spectrum while the relative intensity of the reacted mixture 2859 cm⁻¹ to 2975 cm⁻¹ peaks is 1:2.

To investigate the possibility that the reacted MeOH + SA spectrum in Figure 1b is the spectrum of protonated MeOH, $CH_3OH_2^+$, the spectrum of methanol in HCl was obtained and is shown in Figure 2a,b. The peak assignments are found in Table 1. Methanol is only weakly basic (for $CH_3OH_2^+$; pK_{BH^+} = − 4.86 ± 0.37),[35] and under concentrated acid conditions (4HCl/1MeOH/13H_2O/12M HCl added), 35% of the methanol is protonated.[35] In the Raman spectrum, protonation is observed as a red-shifting of the O−C symmetric stretch from 1034 cm⁻¹ for neat methanol to 1003 cm⁻¹ for protonated MeOH in HCl[35] and 995 cm⁻¹ (small peak) for the MeOH + SA solution as shown in Figure 2a. This shift to lower energy suggests that the O−C bond lengthens as a result of protonation.[36] The decrease in O−C peak intensity for $MeOH_2^+$ of MeOH in HCl and the MHS product of MeOH + SA as compared to the intensity in neat MeOH is mainly due to dilution. (Normalization

Methanol Reaction with Sulfuric Acid

J. Phys. Chem. B, Vol. 108, No. 45, 2004 **17669**
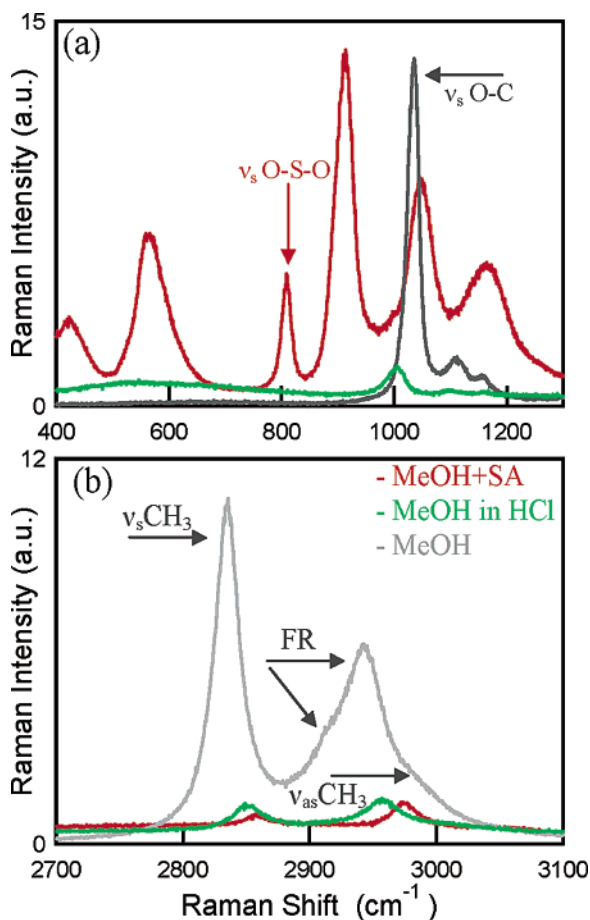
Figure 2. Raman spectra of methanol (grey), methanol in HCl (green), and the reacted mixture of methanol + sulfuric acid (red) (a) from 400 to 1300 cm^{-1} and (b) in the CH$_3$ stretching region (the methanol spectrum in this region has been reduced by a factor of 5).
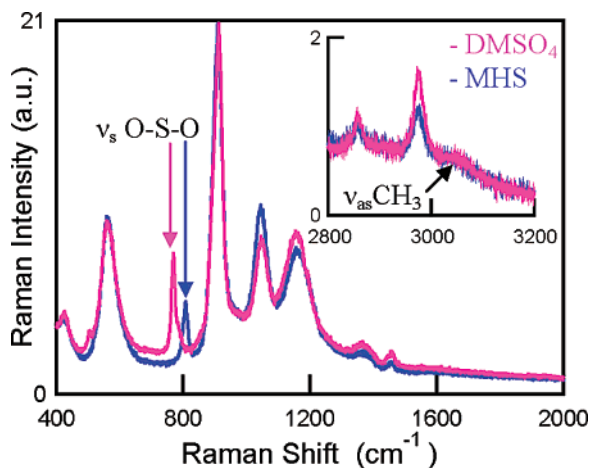
Figure 3. Raman spectra of dimethyl sulfate in sulfuric acid (pink), and methyl hydrogen sulfate in sulfuric acid (blue), from 400 to 2000 cm^{-1} and in the CH$_3$ stretching region (inset).

of the data to equalize the number density produced O—C peaks of comparable intensity.) The reacted MeOH + SA solution spectrum, Figure 2a, has a peak at 808 cm^{-1} not present in the spectrum of MeOH in HCl so it cannot be attributed to protonated methanol.

The CH$_3$ stretching regions of neat methanol, methanol reacted with sulfuric acid, and methanol in hydrochloric acid are compared in Figure 2b. The CH$_3$ stretching region of methanol in HCl is blue-shifted relative to that of neat methanol

but less than that of the reacted mixture. This shift to higher energy for MeOH in HCl indicates that the CH bonds of MeOH are strengthened in HCl. The relative intensity of the symmetric stretch to the higher energy peak has changed from 2:1 to 1:1 for the HCl mixture, and 1:2 for the reacted mixture. The observed decrease in intensity of the CH$_3$ stretching region relative to the MeOH spectrum in Figure 2b is again mainly due to dilution for the MeOH in HCl solution. However, the MeOH + SA solution CH$_3$ region is less intense even after normalization to equalize number density effects (Figure 11b) consistent with the shifting of the CH$_3$ asymmetric stretch to higher wavenumber.

The formation of MHS from the reaction of MeOH with SA has been investigated since the 1950s. The reactions as postulated by Deno and Newman are shown in reactions A—C.[3]

$$ROH_2^+ + H_2SO_4 \rightleftharpoons ROSO_3H + H_3O^+ \qquad (A)$$

$$ROH + H_3SO_4^+ \rightleftharpoons ROSO_3H + H_3O^+ \qquad (B)$$

$$ROH + H_2SO_4 \rightleftharpoons ROSO_3H + H_2O \qquad (C)$$

More recently, the reaction sequence has been expressed by Torn and Nathanson[37] and is shown in reactions a—f.

$$H_2SO_4 + H_2O \rightleftharpoons HSO_4^- + H_3O^+ \qquad (a)$$

$$HSO_4^- + H_2O \rightleftharpoons SO_4^{2-} + H_3O^+ \qquad (b)$$

$$ROH + H_3O^+ \rightleftharpoons ROH_2^+ + H_2O \qquad (c)$$

$$HSO_4^- + ROH + H_3O^+ \rightleftharpoons ROSO_3H + 2H_2O \qquad (d)$$

$$ROSO_3H + H_2O \rightleftharpoons ROSO_3^- + H_3O^+ \qquad (e)$$

$$ROSO_3H + ROH \rightleftharpoons (RO)_2SO_2 + H_2O \qquad (f)$$
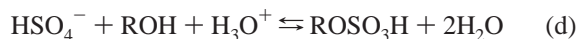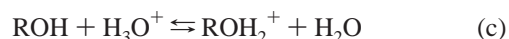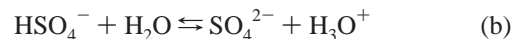
MHS may further react with methanol to form DMSO$_4$ based upon a drop in the desorbing methanol fraction in flow-tube experiments as suggested by reaction f.[1] To confirm the product of the reaction between methanol and sulfuric acid in this study, the Raman spectra of MHS in SA (11SA/1MHS/1H$_2$O) and DMSO$_4$ in SA (12SA/1DMSO$_4$/2H$_2$O) were obtained as shown in Figure 3. Both compounds have a peak in the 800 cm^{-1} region attributed to their singly bonded OSO symmetric stretch, but the positions differ: 769 cm^{-1} for DMSO$_4$ in H$_2$SO$_4$ and 807 cm^{-1} for MHS in SA. Shown in the inset of Figure 3, the 2860 cm^{-1} of MHS and the 2976 cm^{-1} peaks of both MHS and DMSO$_4$ are assigned to CH$_3$ symmetric stretching and Fermi resonance modes, respectively. The 2859 cm^{-1} peak of DMSO$_4$ is assigned to a CH$_3$ symmetric stretch, although it has been previously assigned as a combination band or a Fermi resonance of the CH$_3$ bending mode with the CH$_3$ symmetric stretch.[38] The 3043 cm^{-1} peak of MHS and the 3050 cm^{-1} peak of DMSO$_4$ are assigned to CH$_3$ asymmetric stretches. The CH$_3$ stretching regions of MHS and DMSO$_4$ are shifted to higher wavenumbers relative to that of methanol. The relative intensity of the peaks in the methyl symmetric stretching regions is 1:2, unlike that for neat methanol, but the same as that of the reacted mixture of MeOH + SA. Additional peak assignments are found in Table 1.

The Raman spectra of a series of reacted MeOH + SA mixtures are shown in Figure 4a. The MeOH + SA singly
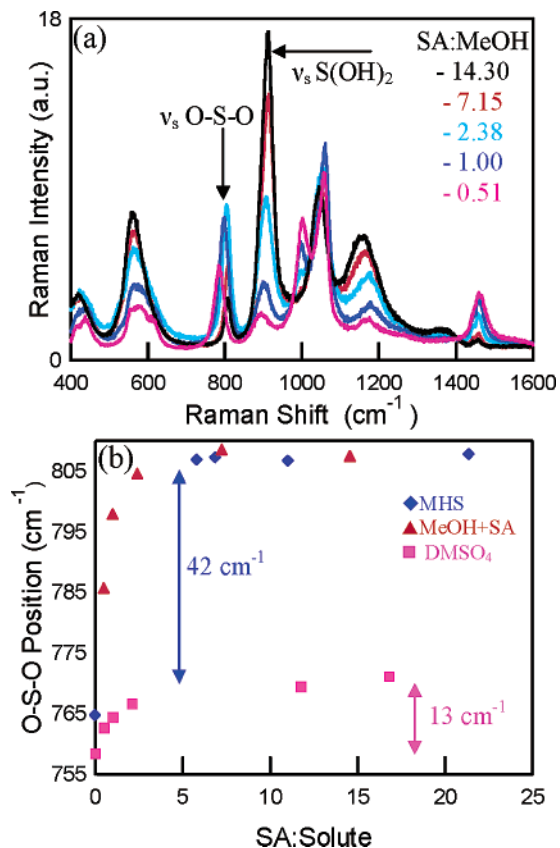
Figure 4. Raman spectra of (a) methanol + sulfuric acid reaction mixtures for various concentrations and (b) the position of the singly bonded OSO symmetric stretch as a function of the ratio of sulfuric acid molecules to solute molecules.

Figure 5. Ab initio calculation schematic of the HOMOs of methyl hydrogen sulfate.

bonded OSO peak at ~800 cm^{-1} shifts with changing SA concentration as shown in Figure 4a. Figure 4b shows the shift of the singly bonded OSO symmetric stretch of DMSO$_4$, MHS, and reacted MeOH with increasing sulfuric acid concentration to higher wavenumber. Shown in Figure 4a, the in-phase S(OH)$_2$ stretch of H$_2$SO$_4$ shifts from 912 cm^{-1} at high SA concentrations to 895 cm^{-1} in low SA concentration, the position of the S(OH) stretch of HSO$_4^-$.[34] The peak at 1043 cm^{-1} is attributed to the ν_s(SO$_3$) of H$_2$SO$_4$ in the largest SA concentration. As the SA concentration decreases, the peak shifts to 1055 cm^{-1}, the peak position attributed to ν_s (SO$_3$) of HSO$_4^-$.[34]

Unlike the 1043 and 912 cm^{-1} bands, the O=S=O stretch at 1153 cm^{-1} does not shift significantly (<5 cm^{-1}) with changing composition (ref 39 and unpublished data from our lab) indicating that the O=S=O stretch is less dependent on the hydrogen bonding. The SA peak shifts indicate that the major sulfuric acid species present in the solution changes from H$_2$-SO$_4$ at high SA to HSO$_4^-$ in lower SA regimes due to protonation of the methanol. In the 0.5SA/MeOH reaction mixture, there is only enough SA to protonate half of the methanol, giving MeOH$_2^+$ + MeOH.

The peak position for the O−C symmetric stretch is ≤1003 cm^{-1} in Figure 4a, indicating the methanol molecules are either protonated or reacted, and partially or fully solvated by sulfuric acid. In ^{1}H NMR studies of CD$_3$OH in SA, methanol is completely protonated in a 1:1 mixture, and the H−H distance in CD$_3$OH$_2^+$ is larger than predicted due to hydrogen bonding.[40] Sulfuric acid has two S−(OH) available for H-bonding and perhaps forms a network involving all the methanol molecules even under the lowest SA concentrations. The O−C symmetric stretch at 1003 cm^{-1} in the 0.5 SA per MeOH reaction
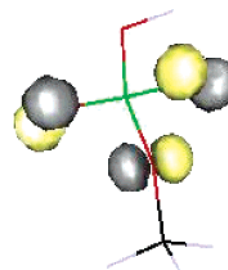
system shifts to lower energy with increasing SA concentration due to O−C bond lengthening as it is solvated more fully by SA. The lengthening of the bond decreases the bond polarizability, and the peak intensity decreases with increasing SA as well.

AM1 calculations suggest that CH$_3$OSO$_3^-$ is solvated by 8−9 H$_2$O molecules.[31] Spectroscopically, this is observed by a change in the position of the vibrational mode affected by the solvation. The solvation of MHS by H$_2$O was investigated here (data not shown) by monitoring the position of the singly bonded OSO stretching peak with increasing H$_2$O excess. The position shifts from 765 cm^{-1} for the crystalline compound to 785 cm^{-1} in a solution of 4 or more H$_2$O molecules per MHS, signifying that one MHS molecule is solvated by four water molecules. The peak position shift is more dramatic in sulfuric acid (Δ ∼ 40 cm^{-1}), Figure 4b, indicating that SA with MHS forms a stronger H-bond network than H$_2$O with MHS. A smaller shift of 5 cm^{-1} is observed for DMSO$_4$ in SA.

Ab initio calculations were performed to aid in understanding the differences between the MHS and DMSO$_4$ solvation shifts. The sulfate moiety of CH$_3$OSO$_3^-$ consists of two doubly bonded oxygens with bond lengths of 1.47−1.48 Å, and a singly bonded oxygen with a bond length of 1.62 Å, in agreement with previous calculations.[31] The HOMO is distributed among these three oxygens, rendering the sulfate moiety available to participate in hydrogen bonding with sulfuric acid. In MHS, CH$_3$OSO$_3$H, the HOMO is predominately on the two doubly bonded O=S moieties and to a lesser extent on the oxygen bonded to the methyl group as shown in Figure 5. The LUMO is on the oxygen of SOH; however, the hydrogen of the SOH may be available for hydrogen bonding to the solvent SA. Again, the sulfate moiety is available for hydrogen bonding. Upon solvation, electron density may be transferred from the O=S bonds of MHS to O−H hydrogen bonds (the MHS oxygen with a SA hydrogen), reducing the electron density around the sulfur atom. The sulfur atom then pulls electron density from the two singly bonded O−S bonds, shortening their length. Spectroscopically, this is observed as a shift to higher energy for the singly bonded OSO ν_s vibration.

These calculations also revealed that the HOMO of DMSO$_4$ is also located on the oxygens of the O=S bonds. However, solvation of DMSO$_4$ by SA is sterically hindered by the presence of two CH$_3$ moieties, reducing the ability of H$_2$SO$_4$ to fully solvate the molecule. This translates as a smaller energy shift for the singly bonded OSO symmetric stretch of DMSO$_4$.

MHS Reaction. Temperature studies were conducted to determine the effect that temperature might have on the extent of reaction, the formation of MHS versus DMSO$_4$, and the effect, if any, on frequency of the product peak. The reaction between MeOH and SA was investigated at −15, 23, and 82 °C.

Methanol Reaction with Sulfuric Acid

J. Phys. Chem. B, Vol. 108, No. 45, 2004 **17671**
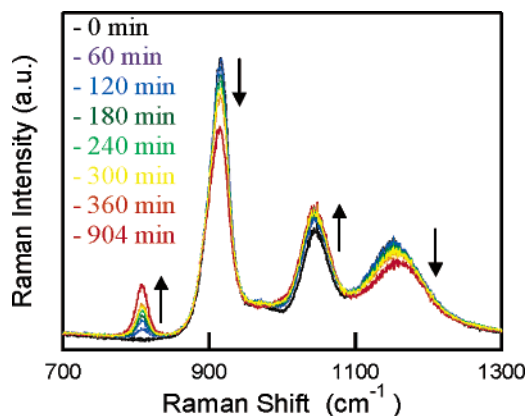
Figure 6. Raman spectra of methanol + sulfuric acid over time (7SA/1MeOH/1H$_2$O at −15 °C).
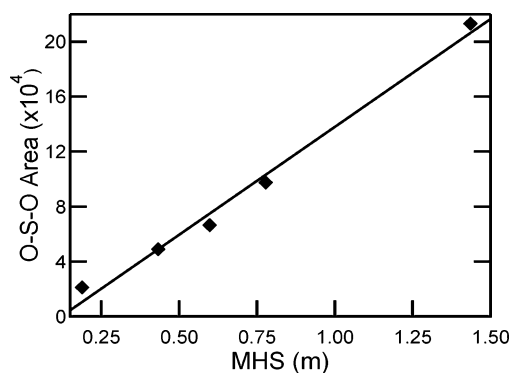
Figure 7. Methyl hydrogen sulfate in sulfuric acid (calculated in molality). The singly bonded OSO symmetric stretch (at ~800 cm^{-1}) peak area is plotted as a function of concentration (diamonds).

Figure 8. (a) Plot of the % yield of methyl hydrogen sulfate as a function of time. The data begins at $t = 60$ min. (b) Plot of [MHS]$_t$/[MeOH]$_t$[H$_2$SO$_4$]$_t$ versus time (min). The slope of the line corresponds to [H$^+$activity]k.

In the low temperature regime, most relevant to middle and upper tropospheric temperatures, the reaction was followed for a 7SA/1MeOH ratio. The Raman spectra were obtained at several times after the initial mixing, and representative spectra are shown in Figure 6. Clearly, the ~800 cm^{-1} MHS product peak is increasing with time as is the peak at 1044 cm^{-1} due to HSO$_4^-$ in the SA/HSO$_4^-$ complex. The peaks at ~912 cm^{-1} due to the in-phase S(OH)$_2$ stretch and the 1153 cm^{-1} peak due to the ν_s O=S=O decrease with time. These observations are consistent with the formation of MHS and related solvent changes from the MeOH + SA reaction. The singly bonded OSO symmetric stretch peak is observed at a higher frequency than the characteristic DMSO$_4$ peak position (Figure 4b), indicating that no DMSO$_4$ is formed (detection limits were determined to be 0.015 m for DMSO$_4$ (~700SA + ~50H$_2$O/1DMSO$_4$)).

To determine the extent of reaction between methanol and sulfuric acid for the low temperature study, the area of the singly bonded OSO symmetric stretch peak of known concentrations of MHS in SA was plotted as a function of concentration as a calibration curve and is shown in Figure 7. According to the reaction sequence, water is also produced as a product and is therefore included stoichiometrically in the calibration curve concentrations. The extent of the MHS calibration curve is limited by the solubility of MHS in SA. The concentration of MHS in the reaction mixture is derived by this method. The data shown in Figure 8a was obtained at (−15 ± 2) °C for initial conditions of 7SA/1MeOH. From Figure 8a, the MHS yield is determined to be (95 ± 2) % for this low temperature study.

From the low temperature experiment, a rate constant was determined from the data plotted in Figure 8a. The rate law used to fit the data has been previously determined[3] and is shown in eq 4.
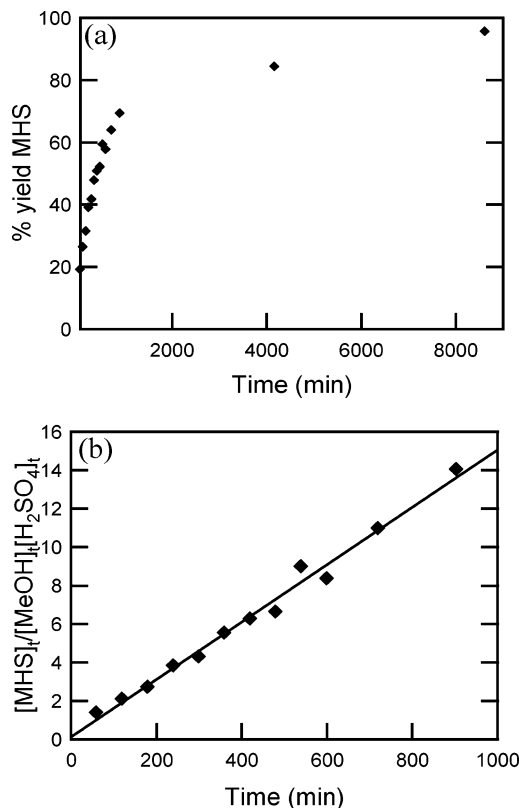
$$\frac{d[ROSO_3H]}{dt} = d[ROH][H_2SO_4][H^+activity] \qquad (4)$$

$$\frac{[MHS]_t}{[MeOH]_t[H_2SO_4]_t} = [H^+activity]kt \qquad (5)$$

Plotting eq 5 as a function of time gives a straight line with a slope corresponding to [H$^+$activity] multiplied by k. The slope of the line is determined to be 0.0149t + 0.1164. (Forcing the intercept through zero gave a slope of 0.0152t.) The value of [H$^+$activity]k is then determined to be 2.48 × 10^{-4} s^{-1}. (Because of the high concentration of the sulfuric acid used in the kinetics studies, the Hammett acidity function cannot be used to determine the activity.)[41] Using an activity for H$^+$ of 7.42[41] produces a rate constant k of 3.4 × 10^{-5} s^{-1}.

This rate constant value is slightly different than that from other experiments that produced values of 69 × 10^{-7} s^{-1} (mol per 1000 g solution)$^{-1}$ in 70.4 wt % SA at 25 °C[3] and 1.9 × 10^{-4} s^{-1} using D$_2$SO$_4$ at an equivalent of 70.62 wt % SA at 25 °C.[42] Increasing the equivalent wt % SA to 77.05 wt % increased the rate constant by a factor of 5 to 9.15 × 10^{-4} s^{-1}.[42] More recently, Knudsen cell studies measured the uptake constants for methanol by SA solutions.[1,2] Kane and Leu[1] measured rate constants of 0.1−10 s^{-1} for methanol uptake at 213 K in 65−80 wt % SA solutions. From uptake measurements, Iraci *et al.*[2] determined a maximum rate constant, $k \le 3 \times 10^{-5}$ s^{-1}, for the reaction between methanol and SA at 72.2 wt % SA for temperatures of 197−223 K. Differences in surface uptake versus bulk reaction, temperature, experimental technique, and/

17672 *J. Phys. Chem. B, Vol. 108, No. 45, 2004*

Van Loon and Allen
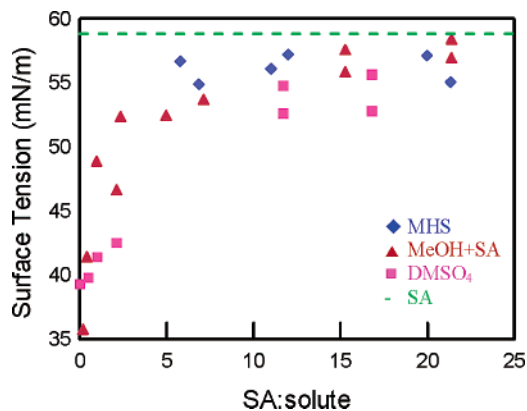
Figure 9. Surface tension measurements of methyl hydrogen sulfate in sulfuric acid (blue diamonds), dimethyl sulfate in sulfuric acid (pink squares), and reaction mixture of methanol + sulfuric acid (red triangles). The surface tension of 96.6 wt % sulfuric acid is shown as a green dotted line.

Figure 10. BBSFG spectra of methanol reduced by a factor of 3 (grey), methanol in HCl (green), the reacted mixture of methanol + sulfuric acid (red), methyl hydrogen sulfate in sulfuric acid (blue), and dimethyl sulfate in sulfuric acid (pink) in the CH$_3$ stretching region.

or sulfuric acid concentration may explain the differences in rate constants.

The low temperature studies did not reveal evidence for the formation of DMSO$_4$. Room temperature and high temperature studies were completed as well to further explore the possibility of DMSO$_4$ production. MHS formation was noted by the presence of the singly bonded OSO symmetric stretch peak at ∼809 cm^{-1}.

For DMSO$_4$ production, neither the room temperature studies nor the high temperature studies provide evidence for DMSO$_4$ formation. However, DMSO$_4$ formation is not necessarily expected without the aid of a catalyst. A search of the literature[43,44] gives several patents for the formation of DMSO$_4$, suggesting high temperatures and the addition of dimethyl ether are required.

Surface Studies. To further understand the reaction of methanol and sulfuric acid as it relates to atmospheric aerosol growth, a surface study with surface tension measurements and sum frequency generation was undertaken. Surface tension data for MeOH + SA, MHS in SA, and DMSO$_4$ in SA at varying SA to solute ratios are presented in Figure 9. As the SA concentration increases, the surface tension measurements tend toward the surface tension of 96.6 wt % SA, suggesting that the alkyl sulfate species are not preferentially segregating to the air−liquid interface particularly at SA/solute ratios greater than 5:1, and that the surface forces resemble those of highly concentrated sulfuric acid. Surface tension measurements of butanol in sulfuric acid−water solutions found similar results and concluded that addition of SA to water suppresses surface segregation of butanol by protonation and conversion to Bu−sulfate species.[37] Also, an ultrahigh vacuum surface study of SA monolayers suggested that propanol segregates into the bulk before undergoing reaction.[45]

Surface vibrational spectroscopy was used to provide insight into the equilibrium surface structures and surface number density. The BBSFG spectrum of the CH region was obtained from the air−liquid interface of neat methanol, MeOH in HCl, DMSO$_4$ and MHS in SA, and the MeOH + SA reaction mixture. (BBSFG spectra of lower spectral regions in particular the 800 cm^{-1} region are planned. Producing short IR laser pulses in this spectral region is nontrivial.) The BBSFG spectrum of neat MeOH is consistent with previously obtained spectra.[12] Peaks observed at 2832 cm^{-1} (fit to 2835 cm^{-1}), 2910 cm^{-1} (fit to 2898 cm^{-1}), and 2944 cm^{-1} (fit to 2847 cm^{-1}) are assigned as
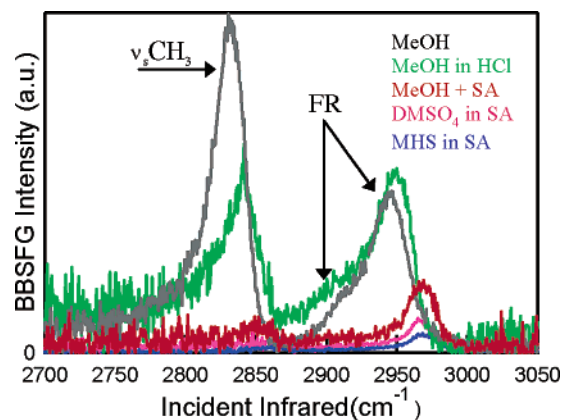
the CH$_3$ symmetric stretch, and the two Fermi resonances. Additionally, a small peak at 2980 cm^{-1} is assigned to the CH$_3$ asymmetric stretch. Methanol at its air−neat methanol interface is somewhat ordered with its methyl groups pointing toward the air phase.[12]

Three peaks are observed for MeOH in HCl at 2840 cm^{-1} (fit to 2843 cm^{-1}), 2920 cm^{-1}, and 2947 cm^{-1} (fit to 2957 cm^{-1}) and are given the same assignments as those for neat MeOH although a fourth peak, the methyl asymmetric stretch, is further shifted to higher energy. Overall, there is a shift to higher energy for MeOH in HCl versus neat MeOH in the BBSFG spectrum shown in Figure 10, which is also observed in the Raman spectrum of Figure 2b. The blue shift is due to shortening of the CH bonds from protonation of the OH group.

The CH stretching regions of MHS, DMSO$_4$, and the MeOH + SA reaction mixture of Figure 10 are shifted to higher energy relative to neat MeOH. The spectra of MHS and DMSO$_4$ in SA are similar, and the reacted mixture MeOH + SA spectrum is comparable to both, with two observed peaks at 2850 cm^{-1} (fit to 2856 cm^{-1}) and 2968 cm^{-1} (fit to 2970 cm^{-1}). Peak assignments are consistent with the Raman assignments. The CH$_3$ asymmetric stretch modes have shifted to higher frequencies relative to neat MeOH and MeOH in HCl.

Polarization BBSFG studies were also conducted to elucidate orientation effects; however, poor signal-to-noise due to small SFG transition moment strengths for the CH$_3$ stretching region only allowed an estimate that the CH$_3$ symmetric stretch transition moment which bisects the CH$_3$ group is somewhat perpendicular to the surface plane. This is based on the intensity ratio of the SSP to the SPS (spectrum not shown here) SFG CH$_3$ symmetric stretching peaks.

There is a decrease in signal intensity of the CH$_3$ symmetric stretch relative to the higher energy Fermi resonance peak for the MeOH in HCl (1:1), the MeOH + SA (1:2), and the MHS (1:2) and DMSO$_4$ (1:2) relative to neat MeOH (2:1). Normalization of the BBSFG spectra in Figure 10 to equalize number density of bulk concentrations reveals interesting changes in the intensity as shown in Figure 11a. These observed intensity changes are dissimilar from the Raman spectra in which the intensities were also normalized to the number density of the solute. The equalized number density Raman spectrum is shown in Figure 11b. In Figure 11a, the MeOH in HCl surface spectrum has the highest intensity, which is consistent with increased ordering of protonated surface methanol in addition to charge effects. The reacted mixture of MeOH + SA normalized surface

Methanol Reaction with Sulfuric Acid

J. Phys. Chem. B, Vol. 108, No. 45, 2004 **17673**
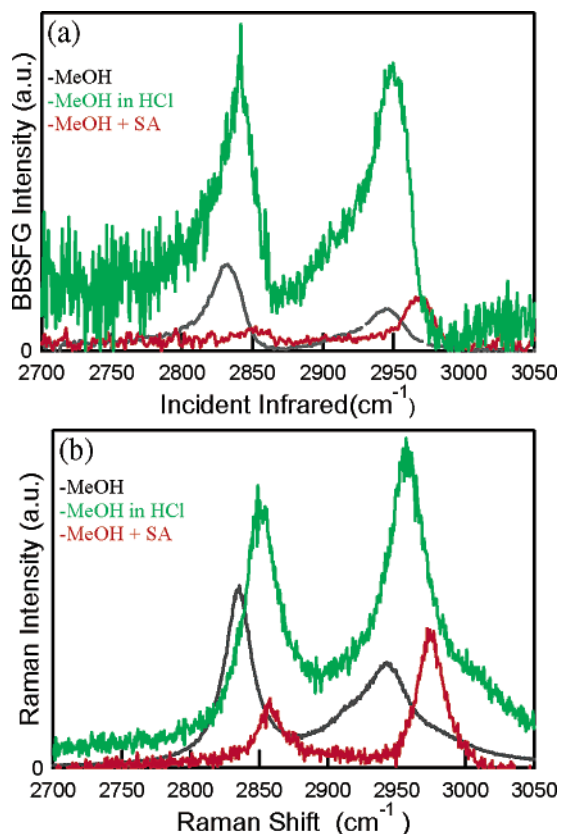
Figure 11. Spectra normalized to equalize the number of solute molecules in order to compare spectral intensities: (a) BBSFG surface spectra, (b) Raman spectra from the bulk solution.

spectrum ((95 ± 5) % conversion to MHS) intensity relative to the neat MeOH normalized surface spectrum is however consistent with the intensity changes observed in the Raman spectrum. The results for the reacted mixture reveal that although the surface tension data suggests that the surface is sulfuric-acid-like, the BBSFG data indicates a similar concentration of the MHS from the reaction mixture in the air−liquid interfacial region relative to the bulk.

Clearly, the reaction of methanol with concentrated sulfuric acid produces MHS with almost complete conversion of available methanol. The MHS product has different physical properties relative to methanol, both in the bulk liquid and at the surface of a solution mixture. Future work in our laboratory is planned to elucidate the protonation of methanol . In the 7SA/1MeOH/1H$_2$O system studied extensively here, it is clear that MHS is the end product, while protonated methanol is likely an intermediate species.

Conclusions

The formation of methyl hydrogen sulfate from the reaction of methanol and sulfuric acid is observed by the presence of a new peak in the Raman spectrum in the 800 cm^{-1} region attributed to the singly bonded OSO symmetric stretch of methyl hydrogen sulfate. The reaction at −15 °C (258 K) using a 7 sulfuric acid to 1 methanol ratio was shown to produce methyl hydrogen sulfate with a (95 ± 5)% efficiency. The rate constant of this reaction was determined to be 3.4×10^{-5} s^{-1}. Dimethyl sulfate, although postulated to be a product of a subsequent reaction of methyl hydrogen sulfate with sulfuric acid, was not observed in these studies.

References and Notes

(1) Kane, S. M.; Leu, M.-T. *J. Phys. Chem. A* **2001**, *105*, 1411.
(2) Iraci, L. T.; Essin, A. M.; Golden, D. M. *J. Phys. Chem. A* **2002**, *106*, 4054.
(3) Deno, N. C.; Newman, M. S. *J. Am. Chem. Soc.* **1950**, *72*, 3852.
(4) Kim, J.; Kim, G.; Cremer, P. S. *J. Am. Chem. Soc.* **2002**, *124*, 8751.
(5) Lambert, A. G.; Neivandt, D. J.; Briggs, A. M.; Usadi, E. W.; Davies, P. B. *J. Phys. Chem. B* **2002**, *106*, 5461.
(6) Ma, G.; Allen, H. C. *J. Am. Chem. Soc.* **2002**, *124*, 9374.
(7) Gaurau, M. C.; Kim, G.; Lim, S.-M.; Albertorio, F.; Fleisher, H. C.; Cremer, P. S. *ChemPhysChem* **2003**, *4*, 1231.
(8) Paszti, Z.; Wang, J.; Clarke, M. L.; Chen, Z. *J. Phys. Chem. B* **2004**, *108*, 7779.
(9) Hommel, E. L.; Ma, G.; Allen, H. C. *Anal. Sci.* **2001**, *17*, 1325.
(10) Hommel, E. L.; Allen, H. C. *J. Phys. Chem. B* **2003**, *107*, 10823.
(11) Hommel, E. L.; Allen, H. C. *Analyst (Cambridge, U.K.)* **2003**, *28*, 750.
(12) Ma, G.; Allen, H. C. *J. Phys. Chem. B* **2003**, *107*, 6343.
(13) Liu, D.; Ma, G.; Levering, L. M.; Allen, H. C. *J. Phys. Chem. B* **2004**, *108*, 2252.
(14) Miranda, P. B.; Shen, Y. R. *J. Phys. Chem. B* **1999**, *103*, 3292.
(15) Shultz, M. J.; Baldelli, S.; Schnitzer, C.; Simonelli, D. *J. Phys. Chem. B* **2002**, *106*, 5313.
(16) Richmond, G. L. *Chem. Rev.* **2002**, *102*, 2693.
(17) Roke, S.; Roeterdink, W. G.; Wijnhoven, J. E. G. J.; Petukhov, a. V.; Kleyn, A. W.; Bonn, M. *Phys. Rev. Lett.* **2003**, *91*, 258302.
(18) Allen, H. C.; Raymond, E. A.; Richmond, G. L. *Curr. Opin. Colloid Interface Sci.* **2000**, *5*, 74.
(19) Allen, H. C.; Raymond, E. A.; Richmond, G. L. *J. Phys. Chem. A* **2001**, *105*, 1649.
(20) Raduge, C.; Pflumio, V.; Shen, Y. R. *Chem. Phys. Lett.* **1997**, *274*, 140.
(21) Wei, X.; Shen, Y. R. *Appl. Phys. B* **2002**, *74*, 617.
(22) Shen, Y. R. *The Principles of Nonlinear Optics*, 1st ed.; Wiley & Sons: New York, 1984.
(23) Hirose, C.; Akamatsu, N.; Domen, K. *Appl. Spectrosc.* **1992**, *46*, 1051.
(24) Hirose, C.; Akamatsu, N.; Domen, K. *J. Chem. Phys.* **1992**, *96*, 997.
(25) Hirose, C.; Yamamoto, H.; Akamatsu, N.; Domen, K. *J. Phys. Chem. A* **1993**, *97*, 10064.
(26) Bain, C. D. *J. Chem. Soc., Faraday Trans.* **1995**, *91*, 1281.
(27) Dick, B.; Gierulski, A.; Marowsky, G. *Appl. Phys. B* **1985**, *38*, 107.
(28) Roke, S.; Kleyn, A. W.; Bonn, M. *Chem. Phys. Lett.* **2003**, *370*, 227.
(29) Brown, M. G.; Raymond, E. A.; Allen, H. C.; Scatena, L. F.; Richmond, G. L. *J. Phys. Chem. A* **2000**, *104*, 10220.
(30) Frisch, M. J.; Trucks, G. W.; Schlegel, H. B.; Scuseria, G. E.; Robb, M. A.; Cheeseman, J. R.; Montgomery, J. A., Jr.; Vreven, T.; Kudin, K. N.; Burant, J. C.; Millam, J. M.; Iyengar, S. S.; Tomasi, J.; Barone, V.; Mennucci, B.; Cossi, M.; Scalmani, G.; Rega, N.; Petersson, G. A.; Nakatsuji, H.; Hada, M.; Ehara, M.; Toyota, K.; Fukuda, R.; Hasegawa, J.; Ishida, M.; Nakajima, T.; Honda, Y.; Kitao, O.; Nakai, H.; Klene, M.; Li, X.; Knox, J. E.; Hratchian, H. P.; Cross, J. B.; Adamo, C.; Jaramillo, J.; Gomperts, R.; Stratmann, R. E.; Yazyev, O.; Austin, A. J.; Cammi, R.; Pomelli, C.; Ochterski, J. W.; Ayala, P. Y.; Morokuma, K.; Voth, G. A.; Salvador, P.; Dannenberg, J. J.; Zakrzewski, V. G.; Dapprich, S.; Daniels, A. D.; Strain, M. C.; Farkas, O.; Malick, D. K.; Rabuck, A. D.; Raghavachari, K.; Foresman, J. B.; Ortiz, J. V.; Cui, Q.; Baboul, A. G.; Clifford, S.; Cioslowski, J.; Stefanov, B. B.; Liu, G.; Liashenko, A.; Piskorz, P.; Komaromi, I.; Martin, R. L.; Fox, D. J.; Keith, T.; Al-Laham, M. A.; Peng, C. Y.; Nanayakkara, A.; Challacombe, M.; Gill, P. M. W.; Johnson, B.; Chen, W.; Wong, M. W.; Gonzalez, C.; Pople, J. A. *Gaussian 03*, revision B.04; Gaussian, Inc.: Pittsburgh, PA, 2003.
(31) Whitfield, D. M.; Tang, T.-H. *J. Am. Chem. Soc.* **1993**, *115*, 9648.
(32) McCreery, R. L. *Raman Spectroscopy for Chemical Analysis*; John Wiley & Sons: New York, 2000.
(33) Hommel, E. L.; Allen, H. C. *Anal. Sci.* **2001**, *17*, 137.
(34) Walrafen, G. E.; Yang, W.-H.; Chu, Y. C.; Hokmabadi, M. S. *J. Solution Chem.* **2000**, *29*, 905.

(35) Weston, R. E., Jr.; Ehrenson, S.; Heinzinger, K. *J. Am. Chem. Soc.* **1967**, *89*, 481.

(36) Solkan, V. N.; Kuz'min, I. V.; Kazanskii, V. B. *Kinet. Catal.* **2001**, *42*, 411.

(37) Torn, R. D.; Nathanson, G. M. *J. Phys. Chem. B* **2002**, *106*, 8064.

(38) Christe, K. O.; Curtis, E. C. *Spectrochim. Acta* **1972**, *28A*, 1889.

(39) Tomikawa, K.; Kanno, H. *J. Phys. Chem. A* **1998**, *102*, 6082.

(40) Batamack, P.; Fraissard, J. *Colloids Surf., A* **1999**, *158*, 207.

(41) Marziano, N. C.; Tomasin, A.; Tortato, C.; Isandelli, P. *J. Chem. Soc., Perkin Trans. 2* **1998**, 2535.

(42) Vinnik, M. I.; Kislina, I. S.; Kitaigorodskii, A. N.; Nikitaev, A. T. *Izv. Akad. Nauk SSSR, Ser. Khim.* **1987**, 2447.

(43) Song, J.; Lu, T.; Mao, C. Preparation of dimethyl sulfate from low concentration sulfur trioxide; Xinghua Pharmaceutical Factory, Shangdong Province, People's Republic of China, 1987.

(44) Xu, F. *Pige Huagong* **2000**, *17*, 39.

(45) Guldan, E. D.; Schindler, L. R.; Roberts, J. T. *J. Phys. Chem.* **1995**, *99*, 16059.

(46) Bertie, J. E.; Zhang, S. L. *J. Mol. Struct.* **1997**, *413−414*, 333.

(47) Gillespie, R. J.; Robinson, E. A. *Can. J. Chem.* **1962**, *40*, 658.

(48) Goypiron, A.; de Villepin, J.; Novak, A. *J. Chem. Phys.* **1978**, *75*, 889.

(49) Givan, A.; Larsen, L. A.; Loewenschuss, A.; Nielsen, C. J. *J. Mol. Struct.* **1999**, *509*, 35.

(50) Nash, K. L.; Sully, K. J.; Horn, A. B. *J. Phys Chem A* **2001**, *105*, 9422.

(51) Bertoluzza, A.; Fagnano, C.; Morelli, M. A.; Tosi, R. *J. Raman. Spectrosc.* **1987**, *18*, 77.

(52) Okabayashi, H.; Okuyama, M.; Kitagawa, T.; Miyazawa, T. *Bull. Chem. Soc. Jpn.* **1974**, *47*, 1075.